

---

# Atomic Layer Deposition on Self-Assembled-Monolayers

---

Hagay Moshe and Yitzhak Mastai

Additional information is available at the end of the chapter

<http://dx.doi.org/10.5772/54814>

---

## 1. Introduction

Atomic layer deposition (ALD) is an advanced technique for growing thin film structures. ALD was developed by Tuomo Suntola and co workers in 1974. At first, the method was called Atomic layer epitaxy (ALE). However, today the name "ALD" is more common. The motivation behind developing ALD was the desire to achieve a technique for creating thin film electroluminescent (TFEL) flat panel displays. [1]- [7]

Several types of materials including metals [8], metal oxides [9], metal nitrides [7] and metal sulfides [10] can be deposited into ALD thin films, depending on the precursors used. ALD advantages are: precise and easy thickness control, superior conformality, the ability to produce sharp interfaces, the substrate size is limited by the batch size and straightforward scale up and repetition of the process.[2-4,6] ALD is appropriate for deposition processes which require angstrom or monolayer level control over coating thickness and/or are maintained on complex topographies of the substrate. No other method for thin film creation can get close to the conformality obtained by ALD.[4] ALD also has several limitations. The Achilles' heel of the method is that ALD is a slow process and therefore is not economic for many industrial processes.[2]

Atomic layer deposition controlled film growth is a significant technology for surface chemistry. In the last four decades, ALD has developed into a system used for depositing thin films in a variety of products. For example, ALD is used in microelectronic production, construction of optical and magnetic devices, flat panel displays, catalysts, and energy conversion including solar cells, utilizing fuel cells, storage batteries or supercapacitors, nanostructures as AFM tips, biomedical purpose and more. [11]

Self Assembled Monolayers (SAMs) are ordered molecular (organic molecules in most cases) assemblies formed by adsorption of molecules on a solid substrate. The surface properties of the surfaces formed are determined by the nature of the adsorbed molecules. [12] A typical surfactant molecule for SAMs is built from three main parts. The first part has a high affinity to the solid surface and is called the "headgroup". The headgroup forms a chemical interaction with the substrate. While adsorbing, the molecules make an effort to adsorb at all surface sites, resulting in a close-packed monolayer. The second molecular part is the alkyl chain. The Van der Waals interactions between these chains cause the SAMs to be ordered. The third part which is exposed at the surface is called the "terminal group". The chain can be terminated with several different groups e.g.  $\text{CH}_3$ , OH, COOH or  $\text{NH}_2$ , allowing the SAMs to be applied for the modification of surface properties. Thus, SAMs can modify the surface free energies of the substrates, ranging from reactive, high energies, to passive, low energies. [12],[13]

This book chapter will focus on a new application of ALD as a novel method for thin film deposition on SAMs. Since ALD is very sensitive to surface conditions, it is an ideal method for film deposition on SAMs. Examples for the application of ALD on SAMs are, for instance, surface patterning and selective deposition of thin films. ALD is a very suitable method for the deposition of thin films with three dimensional structures.[8] This book chapter will cover the most recent and novel applications of ALD used for the preparation of chiral nanosized metal oxide films using chiral SAMs.

### 1.1. Principle of technique

ALD is a Chemical vapor deposition (CVD) process with self-limiting growth and is controlled by the distribution of a chemical reaction into two separate half reactions; the film is done in a growth cycle. Throughout the process, the precursor materials have to be separate. A growth cycle includes four stages: 1) Exposure of the first precursor, 2) purge of the reaction chamber, 3) exposure of the second precursor, and 4) a further purge of the reaction chamber [2,5] (Figure 1). In the first stage, the first precursor reacts with all the sites on the substrate receiving a single molecular layer of the first precursor. The second stage consists of Argon flowing and pumping of the residue of the first precursor to avoid unwanted gas phase reactions between precursors, a reaction which will prevent acceptance of a single molecular layer. In the third stage, the second precursor reacts with one molecular layer of the first precursor to get a single molecular layer of the target material. The fourth stage consists of pumping the residuals of the second precursor [2,5,6]. The cycle ends after four stages. The film thickness is determined by the number of cycles because one cycle deposits one molecular layer (Figure 2). [9] Every stage in the process has to be fully completed before the next stage starts. This means that all the sites on the substrate must react with the precursor and the extra precursor molecules must be removed. The molecular size of the precursor determines the film thickness per cycle. The film density obtained depends on the molecular volume of the precursor- that is to say, a molecule with steric hindrance will probably prevent the formation of a monolayer while small molecules without steric hindrance will allow the formation of a full monolayer. The density of the reactive sites on the substrate is also significant for the nature of the film obtained. One

cycle can take from half a second to a few seconds depending on the reactivity between the gas precursors and the solid substrate. In ALD, spontaneous reactions are desired. [2], [5], [6]

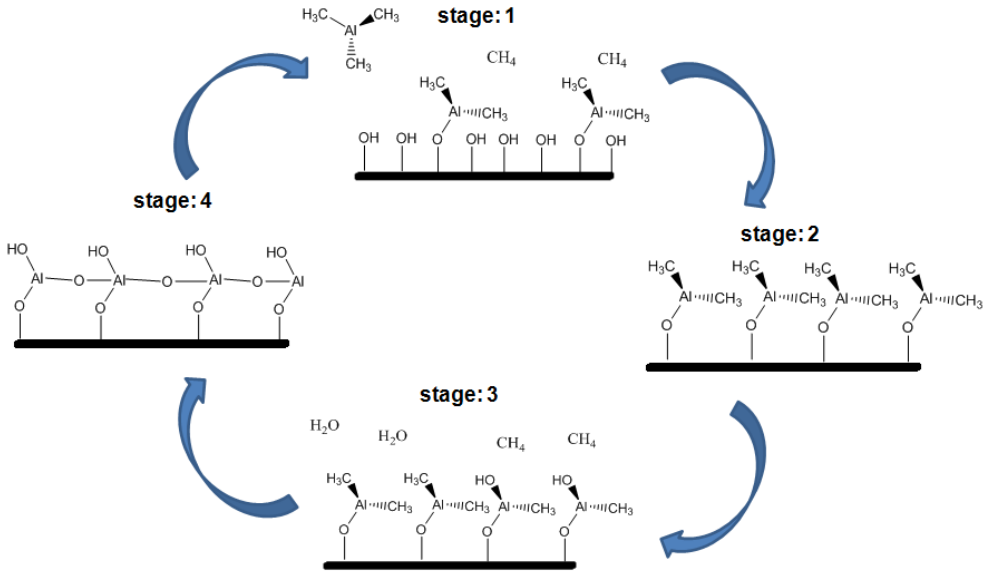


**Figure 1.** ALD growth cycle includes four stages: 1) Exposure of the first precursor, 2) purge of the reaction chamber, 3) exposure of the second precursor, and 4) a further purge of the reaction chamber.

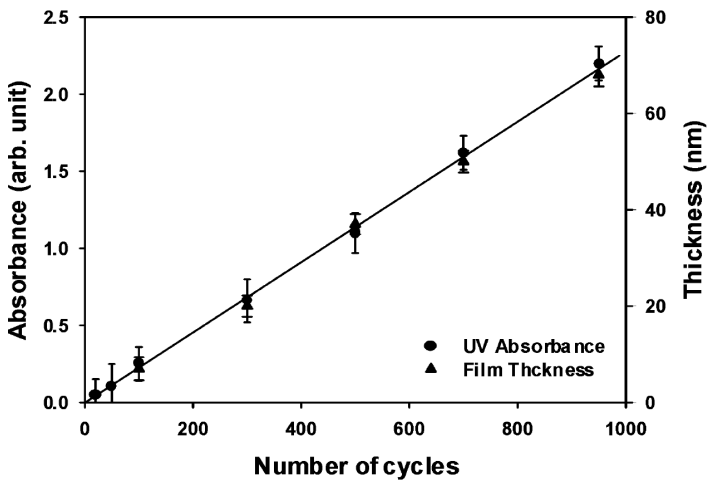


**Figure 2.** UV absorbance and thickness of the TiO<sub>2</sub> thin films versus the number of ALD cycles. [9]

Depending on the precursors used, ALD can deposit several types of materials, including metals as Pt<sup>14</sup>, Ru<sup>15</sup> and Ir<sup>16</sup>; metal oxides as ZnO<sup>17</sup>, TiO<sub>2</sub><sup>9</sup>, ZrO<sub>2</sub><sup>18</sup> and HfO<sub>2</sub><sup>19</sup>; metal nitrides as Hf<sub>3</sub>N<sub>4</sub><sup>20</sup> and Zr<sub>3</sub>N<sub>4</sub><sup>20</sup>; metal sulfides as PbS<sup>10</sup> and Polymers as Polyimide [16]. Using the right precursor is one of the keys for a successful ALD process. Good ALD precursors have to include a number of properties during deposition conditions. First, they have to be stable, evaporable and react with the substrate to completeness. In addition, they must be safe, non toxic and inexpensive. Finally, there should be no etching of the substrate or the growing film and inert volatile byproducts. [2,5-7]

The material type of ALD thin films depends on the precursor type. Normally halides, alkyl compounds, and alkoxides are used as metal precursors. Nonmetal precursors include water, hydrogen peroxide, and ozone for oxygen; hydrides for chalcogens; ammonia, hydrazine, and amines for nitrogen; hydrides for the fifth group in the periodic table. [2], [5]

ALD precursors can be in any state of matter- gas state, liquid state, or solid state. In order to have an effective feeding of precursor molecules to the system, vapor pressure should be high enough. The precursor is also heated sometimes. There must be enough precursors to cover all sites on the substrate surface. [2], [5]- [7]

## 1.2. Advantages and disadvantages

The ALD technique has a number of advantages: ALD has angstrom or monolayer level control on thickness, the film thickness depends only on the number of reaction cycles. ALD has large area deposition ability, the area size depends only on the ALD chamber size. ALD is a very suitable method for the deposition of thin films with three dimensional structures. [8] As a result, ALD has excellent conformality to substrate surfaces. ALD is a reproducible process, can work on low temperatures and uses highly reactive precursors. The ALD method allows processing of different materials in a continuous process. [2], [5], [7]

ALD's weak point is its slow growth rate; one monolayer is deposited per cycle. The monolayer thickness is a few angstroms; if a cycle takes a few seconds, micron thickness deposition will take a few hours. Consequently, ALD is not a useful method for many applications. The growth of films in micrometer size takes too long for ALD to be an economic industrial process. This problem is sometimes overcome by using a big chamber to be able to contain many substrates per batch, but a single wafer process is still more ideal. ALD is an unselective process. Generally, precursor molecules react with all surfaces. In order to achieve selectivity control, pretreatment is necessary. The places which should not be deposited on have to be passivated. As a chemical process, ALD has a risk of impurities. The impurities can come from gas precursors and/or a carrier gas, the process requires material with a high degree of cleanliness. Impure chemicals can lead to the incorporation of impurities and to the growth of poor quality films. [2], [5], [7]

## 1.3. ALD process at low temperature

The ability to perform ALD at low temperatures (ALD-LT) is very important. It is critical for ALD on SAMs and it is the subject of this chapter. SAMs as well as polymers or biological

samples are thermally sensitive materials. At high temperatures, they decompose. [3] In the case of SAMs, there is also desorption from the surface. Inter-diffusions of materials occur at high temperature processes, it has a devastating effect on nano-structured devices. ALD at low temperatures avoids these effects. To carry out ALD-LT, a catalyst is sometimes used [3], [21], [22] although there are reactions that occur without catalysts. [3], [23] Nanostructures of biological structures have very interesting effects. For example, a lotus leaf shows highly hydrophobic behavior due to its nanostructures. The coat of the lotus leaf can be copied by ALD-LT, achieving similar effects. ALD-LT was also used on a tobacco mosaic virus (TMV) on protein spheres [24] and on cellulose fibers from filter paper. [3], [25]

## 2. ALD on self-assembled-monolayer

The use of ALD for depositing thin films onto different SAMs has great potential applications. SAMs are thin organic films which form spontaneously on solid surfaces. The SAM head group has to connect to the substrate strongly enough for stable monolayers to form. Typical SAM head groups are alkanethiols  $[X-(CH_2)_n-SH]$  which are formed on metal surfaces such as Ag, Au, and Cu, and alkyltrichlorosilanes  $[X-(CH_2)_n-SiCl_3]$  formed on  $SiO_2$ ,  $Al_2O_3$ , and other oxide surfaces. [26]- [28]

In general, SAMs are formed by immersing the substrates into a solution comprising the precursor molecules or by bringing the SAM precursors to the substrate surface as vapors. [16] SAMs are well known to modify the physical and chemical properties of surfaces. The surface features can be controlled by using the appropriate SAM. Potential applications include control of wetting and friction behaviors, passivating layers, protection of metals against corrosion, preparation of chiral surfaces, molecular electronics, chemical sensing, soft lithography and more. [10], [26], [29] Figure 3 shows water droplet angle measurements demonstrating the formation of hydrophobicity by ODTS (octadecyltrichlorosilane) SAM on originally hydrophilic  $SiO_2$ . [26]

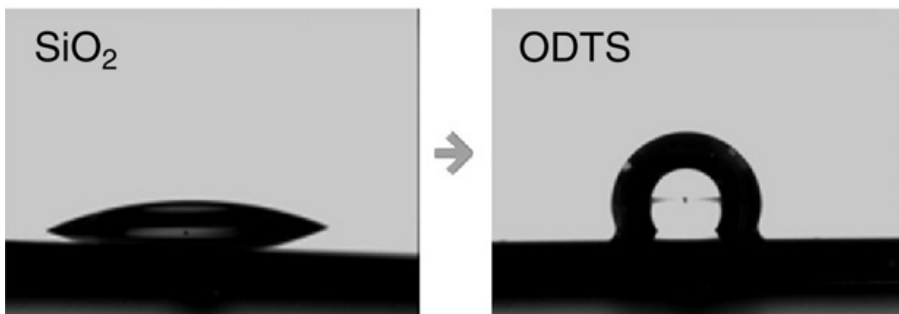


**Figure 3.** Contact angle measurements showing the control of surface energy by ODTS SAM before and after treatments on  $SiO_2$  substrate. [26]

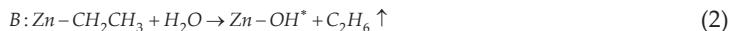
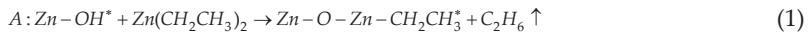
ALD onto SAMs is interesting because the ordered structure of the monolayer can act as a template for the growth of structured thin films. The SAM can be used to engineer the properties of the interface to the original substrate, when the ALD coatings are protecting the SAM. [30]

The thermal stability of the SAMs under the ALD process conditions is very important because of the potential loss of ordering at elevated temperatures. In order to maintain the SAM order during the growth of the ALD film, the ALD process must be done under conditions which are compatible with the thermal budget of the underlying SAM film. [30]

### 2.1. Area-Selective ALD on SAM

Patterned SAMs are commonly used as growth-preventing masks for selective-area ALD. Selective-area ALD is the growth of thin films on the substrate surface on designated sites only. Selective-area ALD requires that the chosen regions of the surface are inert to ALD precursors. In this case the function of the SAM is to protect the surface against deposition. ALD grows only on areas without a SAM, on the desired sites of the surface [16]. High-resolution patterns can be created by printing SAMs by means of soft lithography, [31]- [33] or by removing SAMs using electron beams, [34] ion beams, photolithography, [35] or scanning probe microscopy. [36] Generating patterned SAMs in the most economical way is a critical necessity for using patterned SAMs in advanced applications. Photolithography can transfer an entire pattern on a photomask to a SAM at a given time. Therefore, it is the most practical among various patterning methods. [18]

During the past decade, several groups have used SAMs as a chemical resist to block various ALD precursors, including ZnO [17] [37], TiO<sub>2</sub>[9], [38]- [40], ZrO<sub>2</sub> [18], HfO<sub>2</sub> [19], [41]- [45], Ru [15], Ir [16], [40], [46], Pt [14], [42], [45], [47]- [49], PbS [10] and Polyimide [16]. In 2001 Yan et al. reported on selective area ALD growth of ZnO, they used a microcontact printing (or  $\mu$ CP) with poly(dimethylsiloxane) (PDMS) stamp as a soft lithographic technique. PDMS creates a hydrophobic surface in the stamped area, leaving the ink-free hydrophilic surface unmodified. The pattern consists of arrays of cylinders having cross sectional diameters ranging from 1.0–40  $\mu$ m with center-center distances of 100  $\mu$ m. As ALD precursors they used diethylzinc (DEZ) and deionized water. The deposition process for ZnO consists of two self-limiting chemical reactions, repeated in alternation (ABAB...). Each AB reaction cycle deposits a single monolayer of ZnO, [50] as shown in Eqs. (1) and (2), where asterisks indicate the outermost surface functional groups.



The deposition was carried out at a substrate temperature of 125 °C. The exposure times for DEZ and water vapor were 0.7 sec and 0.5 sec, respectively. ZnO nucleation and growth do

not occur on the; 2 nm thick SAM-patterned areas, but only on the bare, hydrophilic unpatterned areas as illustrated in Figure 4. [17]

Park et al. reported on a patterning method of TiO<sub>2</sub> thin films using microcontact printing of alkylsiloxane SAMs, followed by selective atomic layer deposition of the TiO<sub>2</sub>. Park et al. approach consists of two key steps. First, the patterned alkylsiloxane SAMs were formed by using microcontact printing. Second, the TiO<sub>2</sub> thin films were selectively deposited onto the SAM-patterned Si substrate by atomic layer deposition. [9]

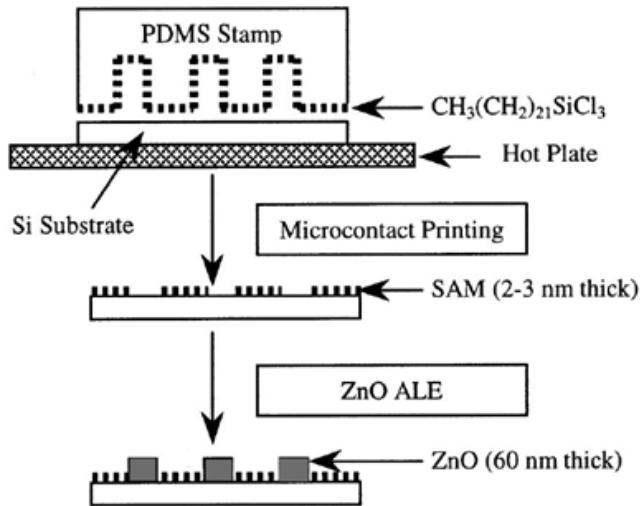


**Figure 4.** Schematic outline of the patterning and deposition procedures used for selective area ZnO thin film growth. [17]

Seo et al. reported on a patterning method for TiO<sub>2</sub> thin films using microcontact printing of alkanethiolate SAMs on gold, followed by selective atomic layer deposition of the TiO<sub>2</sub>. Seo et al. approach consists of three key steps. First, patterned CH<sub>3</sub>-terminated alkanethiolate SAMs on gold were formed by using microcontact printing. Second, the remaining regions of gold were coated with OH-terminated alkanethiolate SAMs. Third, the TiO<sub>2</sub> thin films were selectively deposited onto the SAM-patterned gold substrate by atomic layer deposition. [38] Both groups used PDMS stamp as a soft lithographic technique and same conditions for the preparation of TiO<sub>2</sub> thin films. As ALD precursors they used Titanium isopropoxide (Ti(OPri)<sub>4</sub>) and deionized water. The Ti(OPri)<sub>4</sub> and water were evaporated at 80 and 20 °C, respectively. The cycle consisted of 2 sec exposure to Ti(OPri)<sub>4</sub>, 5 sec Ar purge, 2 sec exposure to water, and 5 sec Ar purge. The total flow rate of the Ar was 20 sccm. The TiO<sub>2</sub> thin films were grown at 100 °C under 2 Torr. The deposition process for TiO<sub>2</sub> also consists of two self-limiting chemical reactions, repeated in alternation (ABAB...). Each AB reaction cycle deposits a single monolayer of TiO<sub>2</sub> [9], [38]. Figure 5 illustrates AFM images and cross sections of micropatterned TiO<sub>2</sub> thin films, which were selectively deposited onto the monolayer-patterned gold substrate by ALD. The patterned SAMs showed high selectivity for TiO<sub>2</sub> ALD;

hence, the patterns of the  $\text{TiO}_2$  thin films were defined and directed by the patterned SAMs generated with microcontact printing. The  $\text{TiO}_2$  thin films are selectively deposited only on the regions exposing the OH groups of the MUO-coated gold substrates, because the regions covered with the ODT monolayers do not have any functional group to react with ALD precursors. These AFM images clearly show that the patterned  $\text{TiO}_2$  thin films retain the dimensions of the patterned SAMs used as templates with no noticeable line spreading. [38]

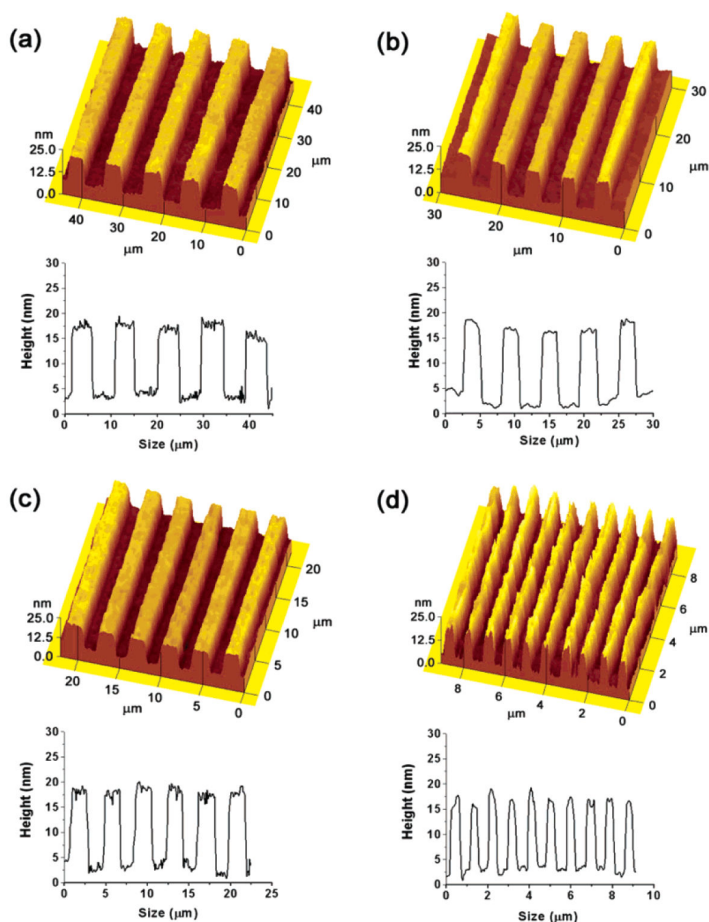


**Figure 5.** AFM images and cross sections of the patterned  $\text{TiO}_2$  thin films generated by using selective ALD on the SAM patterned gold substrates: (a) 3.7  $\mu\text{m}$  lines with 5.6  $\mu\text{m}$  spaces, (b) 1.9  $\mu\text{m}$  lines with 3.7  $\mu\text{m}$  spaces, (c) 1.8  $\mu\text{m}$  lines with 1.9  $\mu\text{m}$  spaces, (d) 0.5  $\mu\text{m}$  lines with 0.4  $\mu\text{m}$  spaces [38].

The successful use of poly(methyl methacrylate) (PMMA) [39] and octadecyltrichlorosilane (OTS) SAMs [40] as a mask layer to obtain the direct patterned deposition of  $\text{TiO}_2$  films has been reported.



Lee and Sung reported on a fabrication method using photocatalytic lithography of octadecylsiloxane SAMs, followed by selective deposition of ZrO<sub>2</sub> thin films using ALD. Lee et al. approach consists of three key steps. First, the alkylsiloxane SAMs were formed by immersing Si substrate in alkyltrichlorosilane solution. Second, photocatalytic lithography using a quartz plate coated with patterned TiO<sub>2</sub> thin films was done to prepare patterned SAMs of alkylsiloxane on the Si substrate. The patterned SAMs of the octadecylsiloxane on the Si substrate were made by using the quartz plate coated with the patterned TiO<sub>2</sub> thin films under UV irradiation in air. The photocatalytic lithography is based on the fact that the decomposition rate of the alkylsiloxane monolayers in contact with the TiO<sub>2</sub> is much faster than that with the SiO<sub>2</sub> under UV irradiation in air. These patterned SAMs define and direct the selective deposition of the ZrO<sub>2</sub> thin films. Third, ZrO<sub>2</sub> thin films were selectively deposited onto the SAMs-patterned Si substrate by ALD. A ZrO<sub>2</sub> thin film was selectively deposited using Zr(OC(CH<sub>3</sub>)<sub>3</sub>)<sub>4</sub> and water as ALD precursors. [18]

Chen et al. investigated a series of self assembled molecules as monolayer resists for HfO<sub>2</sub> atomic layer deposition. A series of n-alkyltrichlorosilanes of chain lengths ranging from 1 to 18 carbon atoms was used to form self-assembled monolayers on the oxide-covered silicon substrates. The ALD precursors for HfO<sub>2</sub> deposition were hafnium tetrachloride (HfCl<sub>4</sub>) and water. The HfO<sub>2</sub> ALD process includes two self-limiting chemical reactions, repeated in alternating ABAB sequences shown in Eqs. (3) and (4), where asterisks indicate the outermost surface functional groups.



Each AB reaction cycle produces an HfO<sub>2</sub> layer terminated by hydroxyl groups, with the hydrochloride byproduct pumped away. After each exposure, the reaction chamber and the gas manifold were purged with nitrogen to avoid possible gas-phase reactions and to eliminate the possible physisorption of the precursors on the substrates. Deposition was carried out at a substrate temperature of 300 °C. The exposure times for HfCl<sub>4</sub> and water vapor were both 2 sec, followed by 3 min of nitrogen purging after each precursor was introduced into the chamber. Chen et al. explained the blocking mechanism by three important factors that influence the blocking efficiency of the monolayer organic films: chain length, tailgroup structure, and headgroup reactivity. This investigation shows that to achieve satisfactory deactivation toward the ALD process, it is crucial to form densely packed, highly hydrophobic organic monolayers. This in turn requires deactivating agents with high reactivity, low steric effect tail groups, and minimum chain length. [19]

Park et al. presented a method that combines SAM passivation and high-k dielectric deposition. Tetradecyl-SAM is formed on a Ge (100) surface via a thermal method. Part of the SAM is then removed by proper annealing, and a HfO<sub>2</sub> film is deposited by ALD. The system development was based on a previous research on the electrical properties of SAMs on Ge

surfaces showing that SAM/Ge interfaces are electrically stable compared to Ge surfaces covered with native oxide. [51] Therefore, a combination of SAM passivation on a Ge surface with high-k gate dielectric deposition is suggested for scaling down gate oxides. [43]

Liu et al. created sub- 10 nm patterns of high dielectric constant (high-k)  $\text{HfO}_2$  on Si substrate, by combining the use of the reassembled S-layer proteins as nanotemplates and an area-selective ALD process. To realize area-selective ALD of metal oxide-based high-k material nanopatterns into the nanotemplates composed of protein architectures, it is necessary to modify the S-layer proteins to introduce different surface functional groups upon them and the silicon substrate surface used in Liu et al. study. As a result, ALD only happens on the Si substrate and cannot take place on the modified surface of the S-layer proteins. ODTS used as an effective monolayer resist on a hydrophilic  $\text{SiO}_2$  surface toward ALD of  $\text{HfO}_2$ , was chosen to modify the surface of the S-layer proteins but not the Si surface. Specifically, the ODTS-modified S-layer proteins are terminated with aliphatic chains ( $\text{R}=(\text{CH}_2)_{17}\text{CH}_3$ ), while the Si surface exposed through the pores defined by the protein units is terminated with -OH or -H functional groups. Since atomic layer deposition has been achieved ideally on surfaces with -OH groups and with an incubation time on surfaces with -H groups, it is therefore feasible to achieve area-selective ALD on a surface with a contrast between aliphatic groups and -OH/-H terminations. [52], [53] ODTS-modified S-layer protein nanotemplate was selectively removed by thermal annealing. Therefore, S-layer proteins reassembled on Si substrate acted as a promising nanotemplate for the sub-10-nm nanopatterning of high-k oxides for future Metal Oxide Semiconductor Field Effect Transistor (MOSFET) applications. [44]

Park et al. demonstrated selective deposition of Ruthenium using contact printed self-assembled monolayer resists by selective area atomic layer deposition. Ruthenium is of interest for advanced metal/oxide/semiconductor (MOS) transistor gate electrodes to reduce polysilicon depletion effects and as nucleation layer for copper interconnect layers. [54] Ruthenium is considered as a viable candidate for p-type MOS devices because it has a vacuum work function near the conduction band edge of silicon, good thermal stability, and low resistivity of the oxidation phase. [55] Selective deposition enables direct formation of  $\text{Ru}/\text{HfO}_2(\text{SiO}_2)/\text{Si}$  capacitor stacks, and the effective work function of ALD Ru is characterized on  $\text{HfO}_2$  and  $\text{SiO}_2$  dielectrics. They used PDMS stamps and OTS SAMs to prepare the patterned organic monolayer. ALD Ru was carried out using bis-(cyclopentadienyl)ruthenium ( $\text{RuCp}_2$ ) as a precursor and dry oxygen.  $\text{RuCp}_2$  is solid at room temperature with vapor pressure of  $\sim 10$  mTorr at the bubbler temperature of  $80^\circ\text{C}$ . The ALD chamber was evacuated to  $5 \times 10^{-6}$  Torr, and the precursor and oxidant gases were introduced into the reactor in separate pulses (3 and 6 sec, respectively) with a 20 sec Ar purge between each reactant. Argon was also used as a carrier gas for the  $\text{RuCp}_2$  pulse. [15]

Färm et al. reported on selective deposition of Iridium by using octadecyltrimethoxysilane (ODS), SAMs prepared from gas phase using a process where water-vapor pulses were given alternately with ODS. SAMs were patterned by a simple lift-off process. [46] In another work, narrow lines of OTS was printed by PDMS stamp which had  $1.5\ \mu\text{m}$  wide print lines and  $1.5\ \mu\text{m}$  wide spaces between. They also presented the passivation of copper surfaces using 1-dodecanethiol ( $\text{CH}_3(\text{CH}_2)_{11}\text{SH}$ ) SAMs against iridium ALD growth. 1-dodecanethiol was

chosen as a SAM precursor because it has relatively long carbon chain, it is liquid and volatile enough so that SAM were prepared from the vapor phase using moderate heating. [16] Iridium was grown only on non-SAM areas at 225 °C from Ir (pentanedione)<sub>3</sub> and O<sub>2</sub>. [16], [40], [46]

Chen and Bent reported on deposition of Pt for the positive patterning area-selective ALD. Pt is a promising electrode material for dynamic random-access memories because of its high chemical stability in an oxidizing atmosphere and its excellent electrical properties. [56], [57] It is also a promising gate metal candidate owing to its high work function (5.6 eV) and compatibility with high-k dielectrics. [58] In the Chen and Bent paper, a deposition of Pt occurs on a SiO<sub>2</sub> film, providing a model process for the deposition of a gate metal on a dielectric. They used 1-octadecene as a monolayer, which undergoes a hydrosilylation reaction selectively on the hydride surface. Following monolayer attachment onto oxide patterned silicon wafers, Pt thin films were selectively deposited onto the substrates. ALD of a Pt thin film was carried out using methylcyclopentadienyl(platinum)trimethyl (CH<sub>3</sub>C<sub>5</sub>H<sub>4</sub>Pt(CH<sub>3</sub>)<sub>3</sub>) and dry air. Exposure times for the Pt precursor and air were 3 and 2 sec, respectively, followed by a 60 and 45 sec N<sub>2</sub> purge after each precursor was introduced into the chamber. The Pt ALD process includes two self-limiting chemical reactions, repeated in the alternating ABAB sequences shown in Eqs. (5) and (6), where asterisks indicate the outermost surface functional groups and OBP, H<sub>2</sub>O, CO<sub>2</sub> are reaction byproducts. [14], [42]

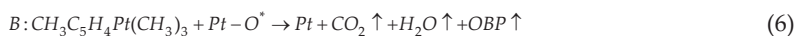
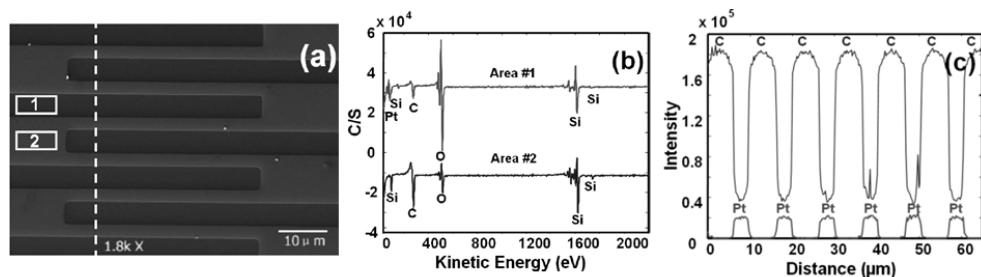


Figure 6 illustrates the Auger electron spectroscopy (AES) analysis of the patterned lines at higher spatial resolution. Figure 6a shows a SEM image of the patterned lines used for the study. In the SEM image, the oxide and the deactivated hydride regions (areas 1 and 2 in Fig. 6.a, respectively) were chosen for AES compositional analysis. The Auger survey scans shown in Figure 6.b reveal that, in the deactivated lines (area 2), the Pt signal is below the AES detection limit (0.5 %), whereas significant Pt is seen in area 1. AES line-scan images that compare the amounts of C and Pt as a function of position are displayed in Figure 6.c. A cross-sectional line (similar to the dashed line shown in Fig. 3a) was obtained perpendicular to the patterned lines. The C and Pt spectra clearly show the alternation as expected, and the edges of the Pt lines are sharp. [14]

Jiang and Bent reported on area selective atomic layer deposition of Platinum on Yttria stabilized zirconia (YSZ) substrates using microcontact printed SAMs. Jianga and Bentb technique can be used to deposit Pt on an YSZ solid oxide electrolyte for the catalyst in solid oxide fuel cell (SOFC). Pt is the catalyst used for a number of reactions, including the O<sub>2</sub> reduction reaction at the cathode of a SOFC, and is especially useful at the lower operating temperatures below (600 °C) that are desired for integratable fuel cell systems. [48], [49]

Lee et al. reported on capability of SAMs to block the deposition of PbS thin films by ALD. ODTs SAMs were chosen to modify the surface termination because of their ability to



**Figure 6.** AES analysis on a patterned structure after the area-selective Pt ALD process: a) SEM image of the patterned area, b) AES selected-area survey composition scan, and c) AES defined line scan. [14]

deactivate ALD reactions as well as their good chemical and thermal stability. Microscale patterns of ALD PbS with high spatial and chemical selectivity were fabricated on ODTS patterned Si/SiO<sub>2</sub> substrates. ODTS was selectively grown only on the oxide patterns defined by the photolithography and deactivated PbS deposition during the ALD process. Hence, materials were selectively deposited by the ALD process only where ODTS was not present. The ALD precursors used were bis(2,2,6,6-tetramethyl-3,5-heptanedionato)lead(II) (Pb(tmhd)<sub>2</sub>) and H<sub>2</sub>S. The base pressure of the ALD chamber was 50 mTorr. The substrate temperature was maintained at 160 °C, and the precursor was sublimated at 140 °C. [59] The PbS ALD process includes two self-limiting chemical reactions, repeated in an alternating ABAB sequence. Lee et al. postulated the following ligand-exchange reactions, which are typical of ALD half-reaction chemistry. In both reactions, a gas-phase precursor molecule reacts with the surface functional species and saturates the entire surface in a self-limiting manner. Each AB reaction cycle produces a PbS layer terminated by sulfhydryl groups, with the corresponding byproducts pumped away. [10]

Färm et al. reported on passivation of copper surfaces for selective-area ALD using 1-dodecanethiol SAMs against polyimide ALD growth. Polyimide is a new material for selective-area ALD and has potential applications as an insulating material in copper interconnects. As test substrates, silicon with evaporated copper dots was used. SAMs were prepared on the copper surfaces from the vapor phase. Polyimide was deposited from 1,2,3,5-benzenetetracarboxylic anhydride (pyromellitic dianhydride) and 4,4'-oxydianiline at 160 °C. [16]

SAMs have typically been created by dipping the solid substrates into a solution containing the precursor molecules. The vapor process is preferred and involves preparing SAMs by bringing the precursors to the substrate surface as vapors. The vapor process has some advantages over the liquid process, e.g., when SAMs have to be formed on three-dimensional structures. The vapor process can prevent problems related to the absorption of liquids into the porous structures. [16] The vapor-phase process also requires fewer precursors than the liquid-phase processes. Moreover, the aggregation of the precursor molecules prior to deposition on the substrate surface, which can cause defects in the arrangement of the SAMs in the liquid-phase process, is significantly reduced using the vapor-phase process. Aggre-

gated precursors had lower vapor pressures than the single-molecule precursors and thus were rarely vaporized. [45] The vapor-phase SAM formation can be carried out in a vacuum system allowing easier combination with the ALD reactor. In principle, SAM formation can be performed in the ALD reactor itself. [45] When SAMs are prepared as an initial stage of the ALD process, the patterning of the SAMs has to be done by relying on the chemical selectivity of the SAM formation. [16] Silane [40], [45], [46] and thiol [16] SAMs has been formed from the vapor phase for selective-area ALD of  $\text{TiO}_2$  [36],  $\text{HfO}_2$  [45], Ir [16], [40], [46], Pt [45] and Polyimide. [16]

The common way to block ALD by using SAMs is limited when the height of the deposited inorganic film exceeds the height of the self-assembled monolayer ( $\sim 2$  nm). In that case the growth will not be area-selective anymore near the interface where the already deposited inorganic film meets the end of the alkyl tails. Near that interface, the ALD reactants are able to adsorb on the inorganic film.

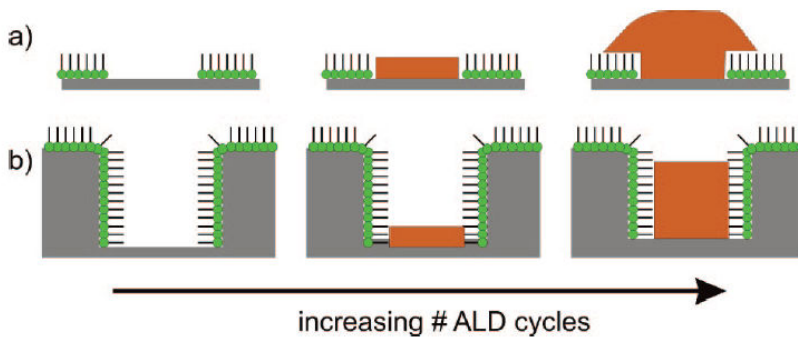


**Figure 7.** (a) Conventional area-selective ALD in which the substrate is planar and contains patterns of self-assembled monolayers. With increasing number of deposition cycles there occurs also sideways film growth originating from adsorption of ALD reactants on the previously deposited ALD film. (b) Blocking the lateral ALD growth independent of deposited film thickness by combining surface modification and topographical features. [37]

The inorganic film is not confined anymore to the original pattern of the SAM and the lateral dimension of the film will increase when more ALD cycles are carried out (see Figure 7.a). Robin et al. have shown a new concept to enable construction of nanoscale lateral structures by area-selective ALD. The concept is based on providing chemical inertness by surface modification combined by nanoscale topographical structures (Figure 7.b). Whereas surface modification, as traditionally used in area-selective ALD, is only a chemical barrier for film growth, Robin et al. shows that the topographical structures are also a physical barrier for film growth. Their concept allows ALD synthesis of constructs that have lateral dimensions many times smaller than the film thickness. Robin et al. used cicada wings as a prototypical example from nature; however, their concept can be also applicable on other types of designed substrates that combine surface modification (including SAMs) with nanoscale topographies. [37]

## 2.2. Surface study by ALD on SAM

Lee et al. studied a surface free energy by atomic layer deposition of  $\text{TiO}_2$  on mixed SAMs. They studied ALD growth modes as a function of surface free energy. [60] Mixed SAMs have been used to modify the surface free energy of the Si substrates. By using solutions containing two different silanes, it formed SAMs containing mixtures of them. The influence of the surface free energy of the Si substrates on the growth modes of  $\text{TiO}_2$  thin films has been studied with AFM, XPS and contact-angle analysis. Mixed SAMs with several surface compositions of  $\text{H}_3\text{C-Si}$  and  $\text{HO-Si}$  were formed on the Si substrates. The surface free energy of the SAM-contact samples was derived from the contact-angle data by using water and diiodomethane, as shown in Table 1. [60]

HO-Si : CH <sub>3</sub> -Si	contact angle $\theta$ [°]		surface free energy [mN/m]		
	water	diiodomethane	$\gamma_s$	$\gamma_s^d$	$\gamma_s^p$
1 : 0	40	25	64	41	22
4 : 1	51	34	56	38	18
2 : 1	62	40	49	36	13
1 : 1	70	45	43	34	9
1 : 2	78	50	38	32	6
1 : 3	89	55	33	31	3
0 : 1	108	60	29	29	0

**Table 1.** Contact angle ( $\theta$ ) and surface free energy ( $\gamma_s$ ) of Si substrates coated with SAMs (d: dispersive part, p: polar part). [60]

The surface free energy of the mixed SAM-contact samples, ranging from 64 to 29 mN/m, appears to be determined primarily by the surface composition of the of  $\text{H}_3\text{C-Si}$  and  $\text{HO-Si}$ , which means that the surface free energy of solid substrate can be controlled by mixed SAMs. The  $\text{TiO}_2$  thin films were grown on the mixed SAM-coated Si substrates by atomic layer deposition from titanium isopropoxide and water. The ALD growth mode of the  $\text{TiO}_2$  film changes as function of the surface free energy of the Si substrates, and the surface free energy can be modified by changing the ratio of the components of the mixed SAMs. A two-dimensional growth mode is observed on the SAM-coated substrates with high surface free energies. As the surface free energy decreases, a three-dimensional growth mode begins to dominate. From the results, Lee et al. have found that the mixed SAMs can be used to control the growth modes of the atomic layer deposition by modifying the surface free energy of the substrates. [60]

Xu and Musgrave used density functional theory (DFT) for investigated surface reactions between trimethylaluminum (TMA) as precursor for alumina and SAMs terminated with different functional groups. [30] They show that the reaction of TMA and the -OH-terminated SAM is favored both thermodynamically and kinetically over the reaction with - $\text{NH}_2$ - and - $\text{CH}_3$ -terminated SAMs. Reactions on the - $\text{NH}_2$ -terminated SAM form more stable complex intermediates; however, because the ligand exchange barrier is large, the precursors are

trapped in the adsorbed complex state. Furthermore, although there is a thermodynamic driving force for this reaction, the reaction is relatively slow compared to the -OH-terminated case and desorption of the precursor is favored over ligand exchange. In the case of the -CH<sub>3</sub>-terminated SAM, there is no thermodynamic driving force for the reaction and the reaction barrier is large. The reaction path and predicted energetics for reactions of TMA and -OH/NH<sub>2</sub>/CH<sub>3</sub>-terminated SAMs as shown in Figure 8. [30]

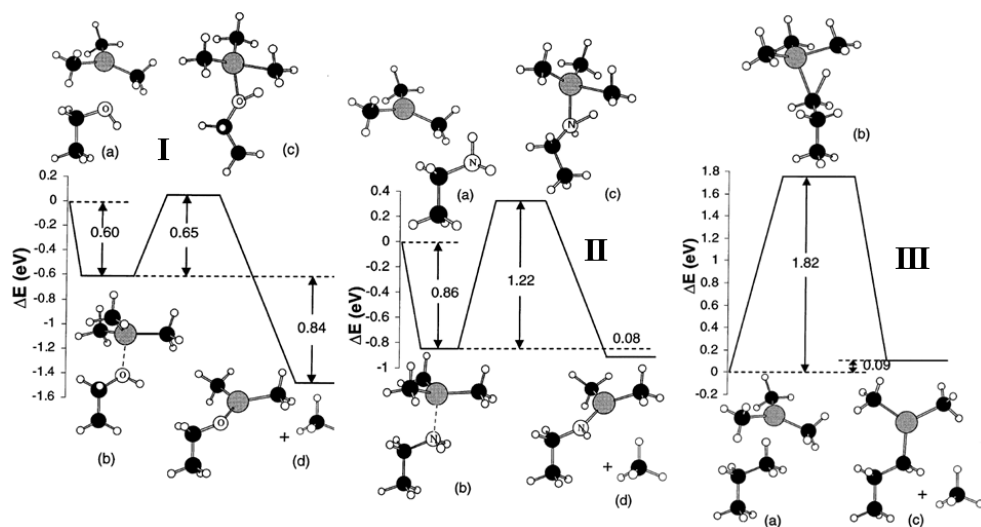


**Figure 8.** I) Reaction path and predicted energetics for reactions of TMA and -OH-terminated SAM. The stationary points correspond to (a) CH<sub>3</sub>CH<sub>2</sub>OH + TMA, (b) complex TMA•OHCH<sub>2</sub>CH<sub>3</sub>, (c) transition state, and (d) CH<sub>3</sub>CH<sub>2</sub>O-Al(CH<sub>3</sub>)<sub>2</sub>+CH<sub>4</sub>. II) Reaction path and predicted energetics for reactions of TMA and -NH<sub>2</sub>-terminated SAM. The stationary points correspond to (a) CH<sub>3</sub>CH<sub>2</sub>NH<sub>2</sub> + TMA, (b) complex TMA•NH<sub>2</sub>-CH<sub>2</sub>CH<sub>3</sub>, (c) transition state, and (d) CH<sub>3</sub>CH<sub>2</sub>NH-Al(CH<sub>3</sub>)<sub>2</sub>+CH<sub>4</sub>. III) Reaction path and predicted energetics for reactions of TMA and -CH<sub>3</sub>-terminated SAM. The stationary points correspond to (a) CH<sub>3</sub>CH<sub>2</sub>CH<sub>3</sub> + TMA, (b) transition state, and (c) CH<sub>3</sub>CH<sub>2</sub>CH<sub>2</sub>-Al(CH<sub>3</sub>)<sub>2</sub>+CH<sub>4</sub>. [30]

The energetics of the reactions does not depend on the length of the SAM using ethyl and pentyl groups as models. [30] After the initial TMA adsorption on the -OH-terminated SAM, the second half-reaction of ALD growth of Al<sub>2</sub>O<sub>3</sub> (Al-CH<sub>3</sub>\*→Al-OH\*) is calculated and the mechanism and energetics are consistent with their previous results for ALD of Al<sub>2</sub>O<sub>3</sub> using TMA and water. [61] Because these adsorption reactions are highly localized, the conclusions are not only limited to the effect of surface functionalization on ALD reactions on SAMs; they can also be extended to reactions on other substrates and to ALD reactions involving other precursors which form dative-bonded complexes. [30]

Lee et al. used DFT simulation for study reactions between Pb(tmhd)<sub>2</sub> precursor to ODTS SAMs and SiO<sub>2</sub>, the results showed an increased activation barrier and a higher overall reaction energy for the Pb(tmhd)<sub>2</sub> precursor on an ODTS-terminated substrate than on a SiO<sub>2</sub> surface. [10]

### 2.3. ALD on chiral SAMs

H. Moshe et al. proposed a new innovative type of stable chiral nanosized metal oxide surfaces. [62] The structure and chirality of this type of chiral surface is based on chiral self-assembled monolayers (SAMs) coated with nanosized films of metal oxide materials deposition by ALD. The idea underlying this new design of nano-chiral surfaces is that the ceramic nanolayers coating the chiral SAMs protects the chiral SAMs that would otherwise be destroyed under the reactions conditions, thereby preserving their enantioselective nature. In Figure 9, the overall structure of the new nanoscale hybrid chiral surfaces based on chiral SAM and ceramic nanolayers is shown.

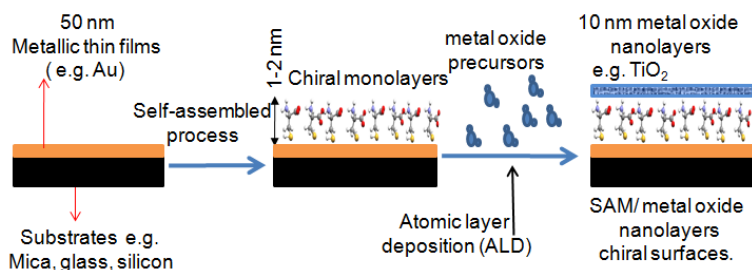


**Figure 9.** Illustration of the design and the synthesis paths for the new chiral SAM/ceramic nanolayers surfaces.

In their study, H. Moshe et al. used TiO<sub>2</sub> to form the protective nanolayers for the chiral SAM since its synthesis does not demand high temperatures that may harm the chiral SAMs. In the research, they utilize the atomic layer deposition (ALD) technique since it provides excellent thickness control and produces very dense and uniform layers. The first step in the synthesis of this type of nano-chiral surface requires the preparation of chiral SAMs. For the chiral SAMs preparation, they used enantiomers of cysteine and glutathione. TiO<sub>2</sub> films were grown by ALD using Ti(N(CH<sub>3</sub>)<sub>2</sub>)<sub>4</sub> and water as the precursors. Their research focuses on evidence of the chirality of the SAM/metal oxide nanosurfaces. Generally, several techniques [63] can be used to study the chiral nature of nano-sized surfaces such as chiral AFM, STM, second-harmonic generation (SHG) and isothermal titration calorimetry. [64] However, due to the unique structure of their nanosized chiral surfaces, they are rather limited in the techniques that can be used to prove the chirality of these surfaces. In their work, H. Moshe et al. have selected several techniques namely quartz microbalance (QMB), second-harmonic generation circular-dichroism (SHG CD) spectroscopy, enantioselective crystallization and chiral adsorption measurements as the methods to study the chirality of the SAM/TiO<sub>2</sub> nanolayer surfaces.

### 3. Conclusions

In this book chapter the preparation, properties and applications of ALD as a novel method for thin film deposition on Self Assembled Monolayers have been briefly reviewed. We have



reviewed a selective-area atomic layer deposition of a variety of materials such as metals, metal oxides, and polymers. First, we presented a brief introduction reviewing the ALD method and principle of operation. Second, we discussed the ability of SAMs to shape the surface of the substrate before the ALD deposition stage. ALD is very sensitive to surface conditions and therefore offers an ideal method for film deposition. Third, we reviewed procedures for properties and applications of ALD on SAMs. We included a variety of molecules and materials and different conditions used for atomic layer deposition. Fourth, we discussed studies which used ALD on SAMs in order to learn surface properties. Finally, a novel application of ALD for the preparation of chiral nanosized metal oxide films using chiral SAMs was discussed. Future work is aimed at the modification and functionalization of surfaces by SAMs used as templates for ALD.

ALD is a technique with high control capabilities. SAMs are a simple and versatile method used for surface design. Integration of the ALD technique and the SAM method can increase the ability to study and engineer substrate surfaces.

## Acknowledgements

H. Moshe would like to acknowledge the Department of Chemistry, Bar Ilan University for funding.

## Author details

Hagay Moshe and Yitzhak Mastai

Department of Chemistry and the Institute of Nanotechnology, Bar Ilan University, Israel

## References

- [1] Suntola, T, & Antson, J. (1977). Method for producing compound thin films. U.S. Patent #4,058,430, Issued Nov. 25
- [2] Leskela, M, & Ritala, M. (2003). Atomic layer deposition chemistry: recent developments and future challenges. *Angewandte Chemie International Edition*, , 42
- [3] Knez, M, Niesch, K, & Niinisto, L. (2007). Synthesis and surface engineering of complex nanostructures by atomic layer deposition. *Advanced Materials*, , 19
- [4] George, S. M. (2010). Atomic layer deposition: an overview. *Chemical Reviews*, , 110
- [5] Ritala, M, & Leskelä, M. (2002). Atomic layer deposition. *Handbook of Thin Film Materials*, Ed.: Nalwa, H. S.) Academic Press, San Diego, , 1, 103-159.

- [6] Niinistö, L, Nieminen, M, Päiväsaari, J, Niinistö, J, Putkonen, M, & Nieminen, M. (2004). Advanced electronic and optoelectronic materials by Atomic Layer Deposition: An overview with special emphasis on recent progress in processing of high-*k* dielectrics and other oxide materials. *Physica Status Solidi (a)*, , 201
- [7] Becker, J. S. (2002). Atomic layer deposition of metal oxide and nitride thin films. Ph.D. dissertation, Harvard University.
- [8] Aaltonen, T. (2005). Atomic layer deposition of noble metal thin films. Ph.D. dissertation, University of Helsinki.
- [9] Park, M. H, Jang, Y. J, Sung-suh, H. M, & Sung, M. M. (2004). Selective atomic layer deposition of titanium oxide on patterned self-assembled monolayers formed by microcontact printing. *Langmuir*, , 20
- [10] Lee, W, Dasgupta, N. P, Trejo, O, Lee, J, Hwang, R, Usui, J, Prinz, T, & Area-selective, F. B. Atomic Layer Deposition of Lead Sulfide: Nanoscale Patterning and DFT Simulations. *Langmuir*, , 26
- [11] Tanskanen, J. T, Bakke, J. R, Bent, S. F, & Pakkanen, T. A. (2010). ALD growth characteristics of ZnS films deposited from organozinc and hydrogen sulfide precursors. *Langmuir*, , 26
- [12] Zaera, F. (2012). The surface chemistry of atomic layer depositions of solid thin films. *The Journal of Physical Chemistry Letters*, , 3
- [13] Ulman, A. (1996). Formation and structure of self-assembled monolayers. *Chemical Reviews*, , 96
- [14] Chen, R, & Bent, S. F. (2006). Chemistry for positive pattern transfer using area-selective atomic layer deposition. *Advanced Materials*, , 18
- [15] Park, K. J, Doub, J. M, Gougousi, T, & Parsons, G. N. (2005). Microcontact patterning of ruthenium gate electrodes by selective area atomic layer deposition. *Applied Physics Letters*, , 86
- [16] Färm, E, Vehkamäki, M, Ritala, M, & Leskelä, M. (2012). Passivation of copper surfaces for selective-area ALD using a thiol self-assembled monolayer. *Semiconductor Science and Technology*, , 27
- [17] Yan, M, Koide, Y, Babcock, J. R, Markworth, P. R, Belot, J. A, Marks, T. J, & Chang, R. P. H. (2001). Selective-area atomic layer epitaxy growth of ZnO features on soft lithography-patterned substrates. *Applied Physics Letters*, , 27
- [18] Lee, J. P, & Sung, M. M. (2004). A new patterning method using photocatalytic lithography and selective atomic layer deposition. *Journal of the American Chemical Society*, , 126
- [19] Chen, R, Kim, H, McIntyre, P. C, & Bent, S. F. (2005). Investigation of self-assembled monolayer resists for hafnium dioxide atomic layer deposition. *Chemistry of materials*, , 17

- [20] Becker, J. S, Kim, E, & Gordon, R. G. (2004). Atomic layer deposition of insulating hafnium and zirconium nitrides. *Chemistry of materials*, , 16
- [21] Gasser, W, Uchida, Y, & Matsumura, M. (1994). Quasi-monolayer deposition of silicon dioxide. *Thin Solid Films*, , 250
- [22] Klaus, J. W, Sneh, O, & George, S. M. (1997). Growth of SiO<sub>2</sub> at room temperature with the use of catalyzed sequential half-reactions. *Science*, , 278
- [23] Luo, Y, Slater, D, Han, M, Moryl, J, & Osgood, R. M. (1997). Low-temperature, chemically driven atomic-layer epitaxy: *In situ* monitored growth of CdS/ZnSe(100). *Applied Physics Letters*, , 71
- [24] Knez, M, Kadri, A, Wege, C, Gösele, U, Jeske, H, & Nielsch, K. (2006). Atomic layer deposition on biological macromolecules: metal oxide coating of tobacco mosaic virus and ferritin. *Nano Letters*, , 6
- [25] Kemell, M, Pore, V, Ritala, M, Leskelä, M, & Linden, M. (2005). Atomic layer deposition in nanometer-level replication of cellulosic substances and preparation of photocatalytic TiO<sub>2</sub>/cellulose composites. *Journal of the American Chemical Society*, , 127
- [26] Kim, H, Lee, H. B. R, & Maeng, W. G. (2009). Applications of atomic layer deposition to nanofabrication and emerging nanodevices. *Thin Solid Films*, , 517
- [27] Laibinis, P. E, Whitesides, G. M, Allara, D. L, Tao, Y. T, Parikh, A. N, & Nuzzo, R. G. (1991). Comparison of the structures and wetting properties of self-assembled monolayers of n-alkanethiols on the coinage metal surfaces, copper, silver, and gold. *Journal of the American Chemical Society*, , 113
- [28] Blum, A. S, Kushmerick, J. G, Long, D. P, Patterson, C. H, Yang, J. C, Henderson, Y. C, Yao, Y, Tour, J. M, Shashidhar, R, & Ratna, B. R. (2005). Molecularly inherent voltage-controlled conductance switching. *Nature Materials*, , 4
- [29] Akkerman, H. B, Blom, P. W. M, De Leeuw, D. M, & De Boer, B. (2006). Towards molecular electronics with large-area molecular junctions. *Nature*, , 441
- [30] Xu, y, & Musgrave, C. B. (2004). A DFT study of the Al<sub>2</sub>O<sub>3</sub> atomic layer deposition on SAMs: effect of SAM termination. *Chemistry of materials*, , 16
- [31] Kumar, A, Biebuyck, H. A, Abbott, N. L, & Whitesides, G. M. (1992). The use of self-assembled monolayers and a selective etch to generate patterned gold features. *Journal of the American Chemical Society*, , 114
- [32] Kumar, A, & Whitesides, G. M. (1993). Features of gold having micrometer to centimeter dimensions can be formed through a combination of stamping with an elastomeric stamp and an alkanethiol "ink" followed by chemical etching. *Applied Physics Letters*, , 63
- [33] Kumar, A, Biebuyck, H. A, & Whitesides, G. M. (1994). Patterning self-assembled monolayers: applications in materials science. *Langmuir*, , 10

- [34] Carr, D. W, Lercel, M. J, Whelan, C. S, Craighead, H. G, Seshadri, K, & Allara, D. L. (1997). High-selectivity pattern transfer processes for self-assembled monolayer electron beam resists *Journal of Vacuum Science & Technology A*, , 15
- [35] Huang, J. Y, & Hemminger, D. A. (1994). Photopatterning of self-assembled alkanethiolate monolayers on gold: a simple monolayer photoresist utilizing aqueous chemistry. *Langmuir*, , 10
- [36] Xu, S, & Liu, G. (1997). Nanometer-scale fabrication by simultaneous nanoshaving and molecular self-assembly *Langmuir*, , 13
- [37] Ras, R. H. A, Sahramo, E, Malm, J, Raula, J, & Karppinen, M. (2008). Blocking the lateral film growth at the nanoscale in area-selective atomic layer deposition. *Journal of the American Chemical Society*, , 130
- [38] Seo, E. K, Lee, J. W, Sung-suh, H. M, & Sung, M. M. (2004). Atomic layer deposition of titanium oxide on self-assembled-monolayer-coated gold. *Chemistry of materials*, , 16
- [39] Sinha, A, Hess, D. W, & Henderson, C. L. (2006). Area-selective ALD of titanium dioxide using lithographically defined poly(methyl methacrylate) films. *Journal of The Electrochemical Society*, G465-G469, 153
- [40] Färm, E, Kemell, M, Ritala, M, & Leskelä, M. (2008). Selective-area atomic layer deposition with microcontact printed self-assembled octadecyltrichlorosilane monolayers as mask layers. *Thin Solid Films* , 517
- [41] Chen, R, & Bent, S. F. (2006). Chemistry for positive pattern transfer using area- selective atomic layer deposition. *Advanced Materials*, , 18
- [42] Chen, R, & Bent, S. F. (2006). Highly stable monolayer resists for atomic layer deposition on Germanium and Silicon. *Chemistry of Materials* , 18
- [43] Park, K, Lee, Y, Im, K. T, Lee, J. Y, & Lim, S. (2010). Atomic layer deposition of HfO<sub>2</sub> on self-assembled monolayer-passivated Ge surfaces. *Thin Solid Films* , 518
- [44] Liu, J, Mao, Y, Lan, E, Banatao, D. R, Forse, G. J, Lu, J, Blom, H. O, Yeates, T. O, Dunn, B, & Chang, J. P. (2008). Generation of oxide nanopatterns by combining self- assembly of S-layer proteins and area-selective atomic layer deposition. *Journal of the American Chemical Society*,, 130
- [45] Hong, J, Porter, D. W, Sreenivasan, R, Mcintyre, P. C, & Bent, S. F. (2008). ALD resist formed by vapor-deposited self-assembled monolayers. *Langmuir*, , 23
- [46] Färm, E, Kemell, M, Ritala, M, & Leskelä, M. (2006). Self-assembled octadecyltrimethoxysilane monolayers enabling selective-area atomic layer deposition of iridium. *Thin Solid Films*, , 12
- [47] Jiang, X, Huang, H, Prinz, F. B, & Bent, S. F. (2008). Application of atomic layer deposition of platinum to solid oxide fuel cells *Chemistry of materials*, , 20

- [48] Jiang, X, & Bent, S. F. (2007). Area-selective atomic layer deposition of platinum on YSZ substrates using microcontact printed SAMs. *Journal of The Electrochemical Society*, 154, DD656, 648.
- [49] Jiang, X, Chen, R, & Bent, S. F. (2007). Spatial control over atomic layer deposition using microcontact-printed resists. *Surface & Coatings Technology*, , 201
- [50] Ott, A. W, & Chang, R. P. H. (1999). Atomic layer-controlled growth of transparent conducting ZnO on plastic substrates. *Materials Chemistry and Physics*, , 58
- [51] Schoell, I. D, Sharp, S. J, Hoeb, M, Brandt, M. S, & Stutzmann, M. (2008). Electronic properties of self-assembled alkyl monolayers on Ge surfaces. *Applied Physics Letters*, , 92
- [52] Chen, R, Kim, H, McIntyre, P. C, & Bent, S. F. (2004). Self-assembled monolayer resist for atomic layer deposition of HfO<sub>2</sub> and ZrO<sub>2</sub> high-κ gate dielectrics. *Applied Physics Letters*, , 84
- [53] Lao, S. X, Martin, R. M, & Chang, J. P. (2005). Plasma enhanced atomic layer deposition of HfO<sub>2</sub> and ZrO<sub>2</sub> high-k thin films. *Journal of Vacuum Science & Technology A*, , 23
- [54] Kim, H. (2003). Atomic layer deposition of metal and nitride thin films: Current research efforts and applications for semiconductor device processing. *Journal of Vacuum Science & Technology B*, , 21
- [55] Zhong, H, Heuss, G, & Misra, V. (2000). Electrical properties of RuO<sub>2</sub> gate electrodes for dual metal gate Si-CMOS. *Electron Device Letters, IEEE*, , 21
- [56] Hiratani, M, Nabatame, T, Matsui, Y, Imagawa, K, & Kimura, S. (2001). Platinum film growth by chemical vapor deposition based on autocatalytic oxidative decomposition. *Journal of The Electrochemical Society*, C524-C527, 148
- [57] Nayak, M, Ezhilvalavan, S, & Tseng, T. Y. (2001). High-Permittivity (Ba, Sr)TiO<sub>3</sub> thin films. *Handbook of Thin Film Materials*, Ed.: Nalwa, H. S.) Academic Press, San Diego, , 3, 99-167.
- [58] Wilk, G. D, Wallace, R. M, & Anthony, J. M. (2001). High-κ gate dielectrics: Current status and materials properties considerations. *Journal of Applied Physics*, , 89
- [59] Dasgupta, N. P, Lee, W, & Prinz, F. B. (2009). Atomic layer deposition of lead sulfide thin films for quantum confinement. *Chemistry of Materials*, , 21
- [60] Lee, J. P, Jang, Y. J, & Sung, M. M. (2003). Atomic layer deposition of TiO<sub>2</sub> thin films on mixed self-assembled monolayers studied as a function of surface free energy. *Advanced Functional Materials*, , 13
- [61] Choy, K. L. (2003). Chemical vapour deposition of coatings. *Progress in Materials Science*, , 48
- [62] Moshe, H, Vanbel, M, Valev, V, Verbiest, T, Dressler, D, & Mastai, Y. Chiral nanosized metal oxide surfaces. unpublished yet.

- [63] Chena, Q, & Richardsonb, N. V. (2004). Physical studies of chiral surfaces. *Annual Reports Section "C"*, , 100
- [64] Shval, A, & Mastai, Y. (2011). Isothermal titration calorimetry as a new tool to investigate chiral interactions at crystal surfaces. *Chemical Communications*, , 47